

Nanowires and Nanoribbons of Charge-Density-Wave Conductor NbSe₃

Y. S. Hor,[†] Z. L. Xiao,^{*†‡} U. Welp,[†] Y. Ito,^{†‡} J. F. Mitchell,[†] R. E. Cook,[†]
W. K. Kwok,[†] and G. W. Crabtree[†]

*Materials Science Division, Argonne National Laboratory, Argonne, Illinois 60439,
and Department of Physics, Northern Illinois University, DeKalb, Illinois 60115*

Received November 22, 2004; Revised Manuscript Received December 12, 2004

ABSTRACT

We report synthesis of nanowires and nanoribbons of the charge-density-wave conductor NbSe₃ through direct reaction of Nb and Se powders. The transverse dimension of the obtained nanostructures, as identified with scanning/transmission electron microscopy, ranges from 20 to 700 nm. X-ray and selected area electron diffraction analyses indicate that these nanowires and nanoribbons are single crystalline. Four-probe resistivity measurements confirm the expected charge-density-wave transitions, and furthermore, we find significant enhancement in the depinning threshold fields, which we attribute to a confinement effect.

Niobium triselenide (NbSe₃) is a low-dimensional inorganic conductor, which shows a variety of nonlinear transport properties associated with charge-density-wave (CDW) phase transitions at 59 and 145 K.^{1–3} NbSe₃ crystals possess a pseudo one-dimensional structure with infinite chains of triangular prismatic units parallel to the *b*-axis.^{4,5} The chains with strong bonding are separated by relatively large distances. As a result, the compound exhibits remarkable anisotropy in most of its physical properties and has been a model system for quasi-one-dimensional CDW studies. Intensive investigations including CDW transport and pinning effects,⁶ structural determination,⁷ NMR,⁸ TEM,⁹ STM,¹⁰ and AFM¹¹ have been performed on pure and doped NbSe₃ crystals. Interest has turned lately to the study of such properties in confined structures. For example, a significant size effect on the threshold field for CDW depinning has been found in micrometer-sized samples.¹² Efforts have also been made to study CDW properties in nanometer-sized samples.^{13–15} Novel collective pinning properties such as dimensionality crossover from two- to one-dimension¹⁵ have been reported including the disappearance of the CDW properties with shrinking sample sizes.¹⁴ The current processes for fabricating nanoscale NbSe₃ samples, however, are relatively inefficient and include two steps. First, bulk NbSe₃ ribbons are synthesized through a standard crystal growth procedure¹⁶ and nanoscale structures are derived from bulk ribbon-like structures with either e-beam lithography followed by plasma etching¹³ or ultrasonic shaking that exploits the weak bonds between chains.¹⁴ These approaches

are either complicated¹³ or can induce defects.¹⁴ Furthermore, these methods can produce only a limited quantity of nanoscale samples.

In this article we report an efficient one-step approach for synthesizing NbSe₃ nanowires and nanoribbons through direct reaction of Nb and Se powders in an evacuated quartz tube. This method provides a simple way to obtain NbSe₃ nanostructures in unlimited quantities. We characterized the structure, morphology, and electronic properties of these NbSe₃ nanostructures. We find that the nanostructures are single-crystalline with high aspect-ratios and exhibit CDW behavior with a larger depinning field than that found in bulk NbSe₃ samples.

Stoichiometric quantities of high purity (>99.99%) niobium and selenium powders with particle sizes of several micrometers were combined. The mixture was ground and sealed in an evacuated quartz ampule of 17 mm in inner diameter and ~15 cm in length, after purging repeatedly with high purity Ar gas to ensure an oxygen free environment. Ampules were then heated to various temperatures, ranging from 580 to 950 °C at the rate of 3 °C/min and maintained at these synthesis temperatures for 1 h before cooling to room temperature at 2 °C/min. We calibrated the furnace temperature where the quartz ampule is located with a type-K (Chromel-Alumel) thermocouple. The temperature stability is about ± 2 °C. Powder X-ray diffraction (XRD) analysis with a monochromatic CuK ($\lambda = 1.540598$) radiation source was used to determine the phase of the product. The morphological and elemental analyses were performed by SEM (Hitachi S-4700-II) and EDS, respectively. A TEM (FEI Tecnai F20ST) equipped with selected area electron diffraction (SAED) attachments was used to obtain structural

* Corresponding author. E-mail: xiao@anl.gov or zxiao@niu.edu.

[†] Argonne National Laboratory.

[‡] Northern Illinois University.

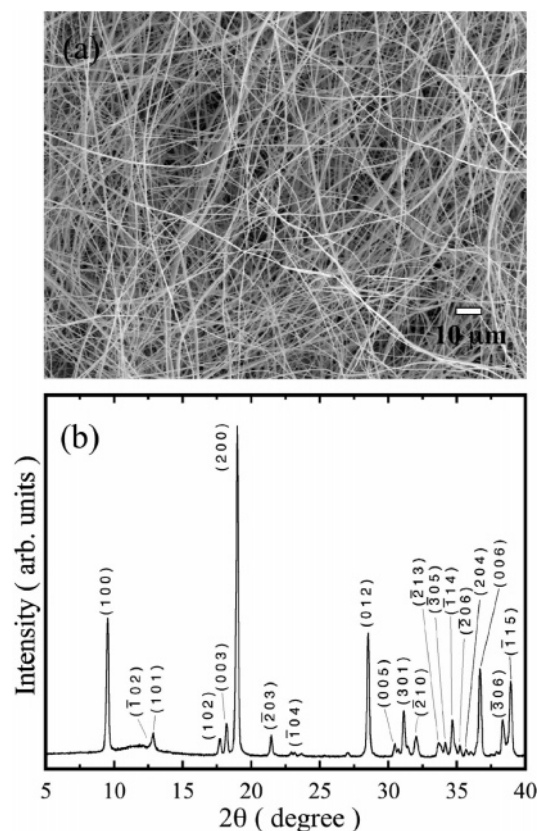


Figure 1. NbSe₃ nanowires synthesized at 700 °C. (a) SEM image and (b) X-ray diffraction pattern.

information on individual nanowires. The CDW properties of these nanostructures were characterized with standard four-probe transport measurements.

We begin by discussing the morphology and structure of the NbSe₃ nanowires synthesized at 700 °C. Figure 1a shows a typical SEM image of the NbSe₃ nanostructures. They are tens of micrometers to a few millimeters in length. Their typical cross-section is rectangular. Following conventional terminology,¹² nanowires (nanoribbons) will be used to refer to the nanostructures with width smaller (larger) than 5 times the thickness. The widths of the synthesized nanostructures range from ~20 nm to ~700 nm, although occasionally, bundles with width up to micrometers can also be observed. The nanoribbons can be as thin as a few nanometers. The XRD pattern, shown in Figure 1b, indicates that the compound is single-phase NbSe₃ with lattice constants consistent with the monoclinic structure reported in the literature (PDF 29-0950).

Figure 2 shows a TEM image (a) of a nanoribbon and its corresponding SAED pattern (b) obtained from an area marked in Figure 2a. This particular nanoribbon is ~230 nm in width and its thickness is estimated to be of the order of 20–30 nm. The contrast of the TEM image is due to the bend contour (diffraction effect). The SAED pattern (Figure 2b) agrees with that of the literature for single crystals.¹⁷ SAED patterns from the entire length of the ribbon display the same patterns except for slight diffraction conditions due to local bending, indicating that the ribbon is a single crystal. NbSe₃ nanowire and nanoribbon axes are parallel to the *b*

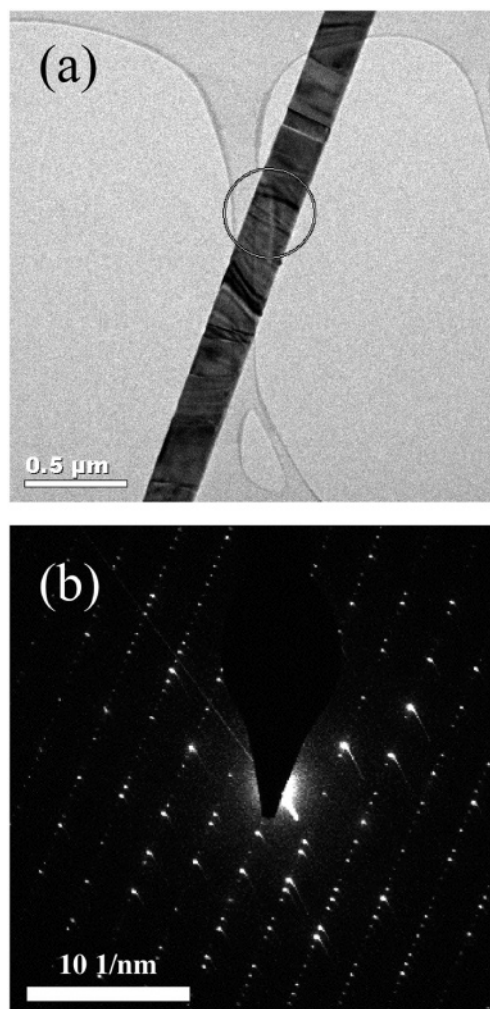


Figure 2. TEM image (a) of a nanoribbon and its corresponding SAED pattern (b) obtained from the marked area in (a).

axis while the smallest dimension of nanoribbons is along the *a* axis.

To explore the synthesis parameters, we synthesized NbSe₃ samples at various Se vapor pressures, heating/cooling rates, sintering times, and sintering temperatures. We found that sintering temperature plays a crucial role in NbSe₃ nanostructure growth while the effects of other parameters are negligible. To study temperature effects, mixtures of Nb and Se powders were heated in an evacuated quartz tube to various temperatures between 580 °C and 950 °C. In each run, identical quartz ampules and equivalent amounts of starting material were used. In all cases, only the sintering temperature was varied while heating and cooling profiles were unchanged. At temperatures above 600 °C, we observed that the ampule filled with brownish Se vapor. The higher the temperature, a thicker Se vapor was observed. During the cooling process, the Se vapor condensed into the compound.

Figure 3 shows the SEM images (left) and XRD patterns (right) of samples sintered at 600, 610, 630, 750, and 850 °C. At 600 °C, XRD shows that the sample consists of Nb₂Se₉ (asterisks) and a small percentage of NbSe₂ (solid circles). The size of the particles is in the micrometer range, as

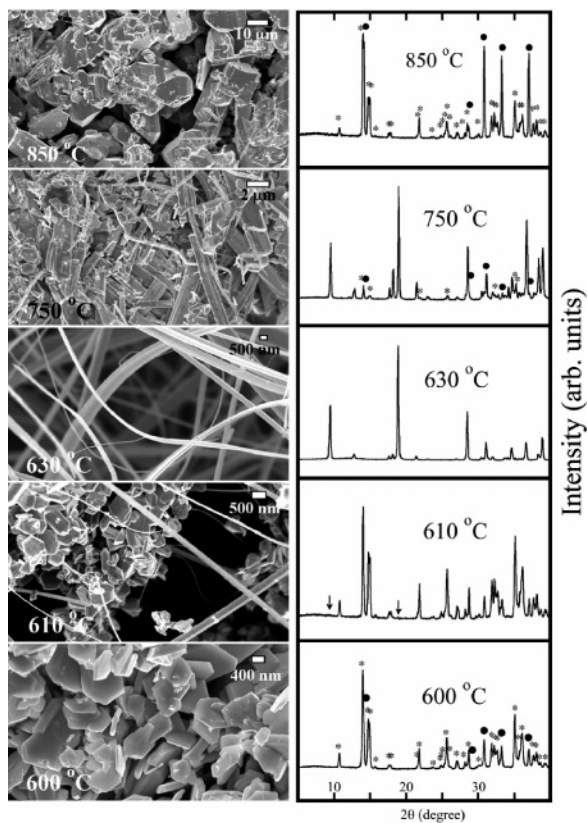


Figure 3. SEM images (left) and XRD patterns (right) of the Nb and Se mixture after sintering at 600, 610, 630, 750, and 850 °C for 1 h. Single phase NbSe₃ can be seen after sintering at 630 °C, while mixed phases of NbSe₂ (denoted with solid circles) + Nb₂Se₉ (denoted with asterisks) form at 600, 610, and 850 °C. At 750 °C we found coexistence of NbSe₂ + Nb₂Se₉ + NbSe₃.

delineated in the SEM image. The NbSe₃ nanowires and nanoribbons begin to grow when the temperature reaches 610 °C, as can be seen from the SEM image. The XRD at 610 °C also reveals a small fraction of monoclinic NbSe₃ phase, as indicated by the arrows, in addition to the majority phases observed in the sample obtained at 600 °C. The cross-section area of the nanostructures increases with increasing sintering temperature and can be seen in the comparison of the SEM image for the 630 °C and the 610 °C compound where the latter shows nanowires as small as 20 nm.

The XRD of the 630 °C compound shows that the NbSe₂ and Nb₂Se₉ phases disappear completely and only the NbSe₃ monoclinic phase exists. The NbSe₃ nanostructures are apparently stable up to ~700 °C. At higher temperatures, the nanostructures begin to decompose. As can be seen from the SEM image for the compound synthesized at 750 °C and 850 °C, the wire-like structures have completely disappeared. Instead, we observed rod- and plate-like microstructures with thickness and length of ~1 μm and ~10 μm, respectively. XRD analyses indicate that the phases in the compound obtained at high temperatures are NbSe₂ and Nb₂Se₉. The amount of NbSe₂ phase increases with increasing sintering temperature, as can be clearly seen from the XRDs for samples obtained at 750 and 850 °C. It is known that NbSe₂ can crystallize into 2H or in 4H structures, which are hard to distinguish with XRD analyses. We conducted

magnetization measurements to detect their superconducting transition temperatures which should be approximately 7 and 6 K for the 2H and 4H phases, respectively. The observed superconducting transition temperature of 7.2 K indicates the NbSe₂ phase obtained here is 2H.

The above results show that the formation of NbSe₃ nanowires and nanoribbons via direct reaction of Nb and Se powders can take place only in a narrow sintering temperature range of 610 °C – 700 °C. We note that free-flowing powder products have been reported in the first stage of bulk NbSe₃ crystal growth where stoichiometric Nb and Se powder mixtures were sintered to form the precursor material.¹⁸ Nath et al. even obtained grayish powder at a sintering temperature of 697 °C from Nb and Se powders.¹⁹ It is conceivable that these products contain NbSe₃ nanowires such as those described here, though it may also be a mixture of NbSe₂ and Nb₂Se₉ phases as well. This slight temperature inconsistency can be caused by the variations in furnace temperature between laboratories.

The vapor–liquid–solid (VLS) mechanism²⁰ proposed by Wagner et al. forty years ago for large whisker growth has been often utilized to grow or to understand the formation of nanowires.^{21,22} In-situ TEM imaging did verify this growth mode with²³ or without²⁴ exotic catalytic metal nanoparticles, by observing the liquid droplets on the head of growing nanowires of Ge²³ and GaN,²⁴ respectively. In the NbSe₃ system, Tsuneta et al. also speculated the self-catalytic VLS growth mechanism for the observed topological microstructures.²⁵ However, careful SEM and TEM imaging on the tips of our NbSe₃ nanostructures reveals no sign of any droplets typically associated with VLS growth. We speculate that the nanowire and nanoribbon formation of NbSe₃ observed here arises due to its unique chained crystal structure, which promotes 1D growth, as demonstrated in the single-crystal growth where 1D ribbons were always obtained.¹⁶

The observation of Nb₂Se₉ + NbSe₂ phases at both ends of the temperature range where NbSe₃ nanostructures are formed is puzzling. This behavior indicates that the Nb₂Se₉ + NbSe₂ phases formed at low temperatures during the heating period can be transformed into NbSe₃ with increasing temperature, while the Nb₂Se₉ + NbSe₂ phases formed at high temperatures are stable relative to NbSe₃ at 610~700 °C during cooling. To explore this interesting phenomenon, we took Nb₂Se₉ + NbSe₂ powders synthesized at 850 °C and heated them in fused silica ampules in the same way as the Nb+Se mixture (3 °C/min to 650 °C; 1 h soak; 2 °C/min cool). In this case, we again observed the conversion of Nb₂Se₉ + NbSe₂ powders into NbSe₃ nanowires. On the other hand, if the Nb₂Se₉ + NbSe₂ powders are cooled to 650 °C and held there for 1 h before final cooling, no NbSe₃ is found. These results lead us to speculate that the NbSe₃ nanowires form only during heating and thus depend on the Se evaporation for their formation. Additional studies will be required to fully understand this phenomenon that is directly related to the NbSe₃ nanostructure formation mechanism.

We turn now to the electronic properties of the synthesized nanostructures. Due to nesting of different parts of the Fermi

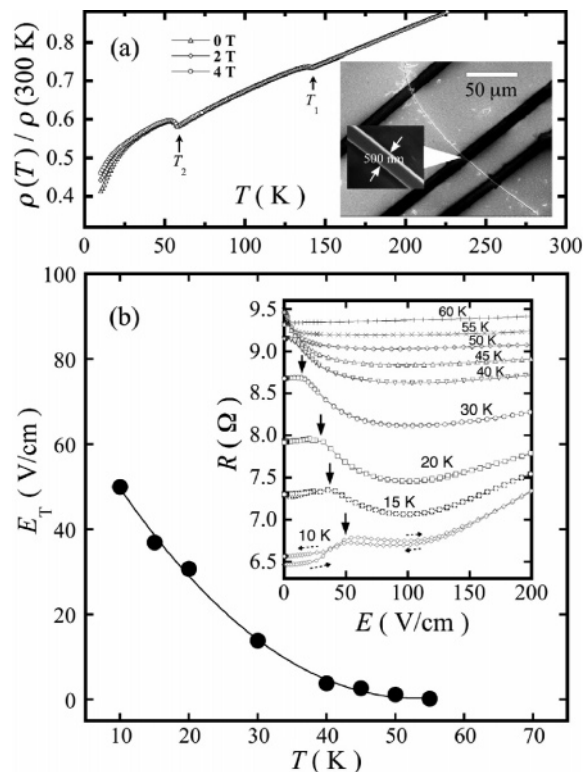


Figure 4. (a) Temperature dependence of the normalized electrical resistivity of a 500 nm wide NbSe₃ nanowire in magnetic fields, $H \perp b = 0, 2,$ and 4 T. The inset shows the four-probe construction of the resistance measurement. Four gold pads (brighter areas) are separated from each other by 12.5 μm gaps (darker areas). The small rectangular box shows the enlarged picture of the wire. CDW phase transitions were identified at $T_1 = 142$ K and $T_2 = 58$ K from the bumps in the resistance versus temperature curve. (b) Temperature dependence of the CDW depinning threshold field E_T for this 500 nm NbSe₃ nanowire. The inset shows R versus E for temperatures at 60 K and below. The dark arrows indicate the threshold field E_T . The dash-lined arrows indicate increasing and decreasing field directions.

surface, bulk NbSe₃ shows two CDW transitions at $T_1 = 145$ K and $T_2 = 59$ K. This electronic character is also observed in our nanowires and nanoribbons. In Figure 4a, we show the temperature dependence of the normalized electrical resistivity of a NbSe₃ nanowire with width of 500 nm in applied magnetic fields, H (perpendicular to b -direction) = 0, 2, and 4 T. The applied electric field for the resistance measurement is ~ 0.02 V/cm. Two resistivity bumps at $T_1 = 142$ K and $T_2 = 58$ K, corresponding to the two CDW transitions, are clearly seen. The size of the resistance anomalies at T_1 and T_2 , which is significantly smaller than typically observed on bulk crystals, is consistent with findings on lithographically generated NbSe₃ nanowires²⁶ for which the charge density wave anomalies were progressively suppressed with decreasing sample cross-section. For zero applied field, the residual resistance ratio, $RRR = R(300\text{ K})/R(10\text{ K})$ is ~ 2 , which is 1 order of magnitude smaller than that obtained from a high-purity micrometer-scale NbSe₃ crystal,¹ but is comparable with that of NbSe₃ nanowires obtained with both e-beam lithography patterning²⁶ and ultrasonic shaking.¹⁴ That is, the small residual resistance ratio is mainly due to the size effect rather

than caused by impurity or defects. In fact, as determined by TEM, the nanowires and nanoribbons grown with this method are single crystalline with low density of defects, as usually expected for samples grown via the vapor approach. There is a positive magnetoresistance MR below $T_2 = 58$ K but no obvious MR at around T_1 and above. However, we observe no shift in the position of the maximum at T_2 and no enhancement of the amplitude as reported elsewhere.²⁷

An interesting feature of the CDW is its collective transport mode. When an electric field is applied, CDWs slide along the direction of the applied field, giving rise to a strongly nonlinear conductivity. Because of the pinning effect, sliding mode conduction can occur only when a well-defined threshold field, E_T , is reached. For some crystals the onset of CDW motion at low temperatures occurs through a sharp, hysteretic switching event.^{28,29} Figure 4b shows the temperature dependence of E_T for the 500 nm sized NbSe₃ wire, and the inset shows the applied field E dependence of resistance R for temperatures below T_2 . The R versus E plot shows that there is no sign of nonlinear conductivity up to electric fields of several hundreds of V/cm at temperature above T_2 . The arrows indicate the onset of depinning at the threshold field E_T . The apparent hysteresis in the $R(E)$ curves at low temperatures is reminiscent of the switching behavior seen in single-crystal samples. We attribute the increase of the resistance at large E and low T to a heating effect during the measurement. We found from Figure 4b that the obtained E_T 's are much larger than those typically observed in crystals. This could imply that our nanowires have a high defect concentration, and therefore higher CDW pinning than typical crystals, an observation that is consistent with the low RRR value. Alternatively, it has been shown^{15,27} that for plate-like crystals E_T increases as $1/t$ once the sample thickness t becomes smaller than the phase coherence length of the CDW. In this limit E_T is determined by 2D collective pinning. For a nanowire sample, E_T is expected to increase as $1/d^3$ (where d is the wire diameter), which could account for the large values observed here. The plot of E_T as a function of temperature follows $E_T \sim \exp(-T/T_0)$ for $T \leq 40$ K, where T_0 is a constant. Our fit yields $T_0 = 16$ K, which is very close to the 17 K observed for wires with a thickness of 300 nm and width between 500 nm and 1 μm.³⁰

In conclusion, we have shown that single crystalline NbSe₃ nanowires and nanoribbons can be synthesized through a one-step direct reaction approach. The growth of NbSe₃ nanostructures occurs in a narrow reaction temperature range of 610~700 °C. Four-probe resistivity measurements showed the expected charge-density-wave (CDW) transitions at $T_1 = 142$ K and $T_2 = 58$ K. The single-step synthesis method described here provides a straightforward access to NbSe₃ crystalline nanowires and nanoribbons that may be extended to other materials in the Nb–Se system. Our results on magnetoresistance, residual resistance ratio, and threshold field indicate that the quality of our readily synthesized NbSe₃ nanostructures is comparable to those fabricated through e-beam lithography or ultrasonic shaking from bulk single crystals.

Acknowledgment. This work was supported by the U.S. Department of Energy, BES-Materials Science, contract no. W-31-109-ENG-38. One of us (Z.L.X.) also acknowledges support from the U.S. Department of Education, the State of Illinois under HECA and the Consortium for Nanoscience Research at Argonne National Laboratory and the University of Chicago. The scanning/transmission electron microscopies were performed in the Electron Microscopy Center at Argonne.

References

- (1) Ong, N. P.; Monceau, P. *Phys. Rev. B* **1977**, *16*, 3443.
- (2) Tsutsumi, K.; Takagaki, T.; Yamamoto, M.; Shiozaki, Y.; Ido, M.; Sambongi, T.; Yamaya, K.; Abe, Y. *Phys. Rev. Lett.* **1977**, *39*, 1675.
- (3) Fleming, R. M.; Moncton, D. E.; WcWhan, D. B. *Phys. Rev. B* **1978**, *18*, 5560.
- (4) van Smaalen, S.; de Boer, J. L.; Meetsma, A.; Graagsma, H.; H-S. Sheu, Darovskikh, A.; Coppens, P. *Phys. Rev. B* **1992**, *45*, 3103.
- (5) Prodan, A.; Jug, N.; van Midden, H. J. P.; Bohm, H.; Boswell, F. W.; Bennett, J. C. *Phys. Rev. B* **2001**, *64*, 115423.
- (6) Thorne, R. E.; Lyons, W. G.; Lyding, J. W.; Tucker, J. R.; Bardeen, J. *Phys. Rev. B* **1987**, *35*, 6348. Ramakrishna, S.; M, Maher, P.; Ambegaokar, V.; Eckern, U. *Phys. Rev. Lett.* **1992**, *68*, 2066. Latyshev, Y. I.; Laborde, O.; Monceau, P.; Klaumünzer, S. *Phys. Rev. Lett.* **1997**, *78*, 919.
- (7) Brock, J. D.; Finnefrock, A. C.; Ringland, K. L.; Sweetland, E. *Phys. Rev. Lett.* **1994**, *73*, 3588. Rouziere, S.; Ravy, S.; Pouget, J. P.; Thorne, R. *Solid State Commun.* **1996**, *97*, 1073. Li, Y.; Noh, D. Y.; Price, J. H.; Ringland, K. L.; Brock, J. D.; Lemay, S. G.; Cicak, K.; Thorne, R. E.; Sutton, M. *Phys. Rev. B* **2001**, *63*, R041103.
- (8) Ross, J. H., Jr.; Wang, Z.; Slichter, C. P. *Phys. Rev. B* **1990**, *41*, 2722. Ross, J. H., Jr.; Wang, Z.; Slichter, C. P. *Phys. Rev. Lett.* **1986**, *56*, 663.
- (9) Steeds, J. W.; Fung, K. K.; McKernan, S. *J. Phys. (Paris), Colloq. C3* **1983**, *44*, 1623. Fung, K. K.; Steeds, J. W. *Phys. Rev. Lett.* **1980**, *45*, 1696.
- (10) Slough, C. G.; Giambattista, B.; Johnson, A.; McNairy, W. W.; Coleman, R. V. *Phys. Rev. B* **1989**, *39*, 5496.
- (11) Gong, Y.; Xue, Q.; Dai, Z.; Slough, C. G.; Coleman, R. V. *Phys. Rev. Lett.* **1993**, *71*, 3303.
- (12) McCarten, J.; Maher, M.; Adelman, T. L.; Thorne, R. E. *Phys. Rev. Lett.* **1989**, *63*, 2841.
- (13) Mantel, O. C.; Chalin, F.; Dekker, C.; van der Zant, H. S. J.; Latyshev, Y. I.; Pannetier, B.; Monceau, P. *Phys. Rev. Lett.* **2000**, *84*, 538.
- (14) Zaitsev-Zotov, S. V. *Microelectron. Eng.* **2003**, *69*, 549. Zaitsev-Zotov, S. V.; Slot, E.; van der Zant, H. S. J. *J. Phys. IV France* **2002**, *12*, Pr9–115.
- (15) Slot, E.; van der Zant, H. S. J.; O'Neill, K.; Thorne, R. E. *Phys. Rev. B* **2004**, *69*, 073105.
- (16) Levy, F.; Berger, H. *J. Cryst. Growth* **1983**, *61*, 61.
- (17) Hodeau, J. L.; Marezio, M.; Roucau, C.; Ayroles, R.; Meerschaut, A.; Rouxel, J.; Monceau, P. *J. Phys. C: Solid State Phys.* **1978**, *11*, 4117.
- (18) Revolinsky, E.; Brown, B. E.; Beerntsen, D. J.; Armitage, C. H. *J. Less-Common Met.* **1965**, *8*, 63.
- (19) Nath, M.; Kar, S.; Raychaudhuri, A. K.; Rao, C. N. R. *Chem. Phys. Lett.* **2003**, *368*, 690.
- (20) Wagner, R. S.; Ellis, W. C. *Appl. Phys. Lett.* **1964**, *4*, 89.
- (21) Morales, A. M.; Lieber, C. M. *Science* **1998**, *279*, 208.
- (22) Holmes, J. D.; Johnston, K. P.; Doty, R. C.; Korgel, B. A. *Science* **2000**, *287*, 1471.
- (23) Wu, Y.; Yang, P. *J. Am. Chem. Soc.* **2001**, *123*, 3165.
- (24) Stach, E. A.; Pauzausjje, P. J.; Kuykendall, T.; Goldberger, J.; He, R. R.; Yang, P. D. *Nano Lett.* **2003**, *3*, 867.
- (25) Tsuneta, T.; Tanda, S. *J. Cryst. Growth* **2004**, *264*, 223.
- (26) Holst, M. A. *Charge-Density Wave Nanowires*; Master's Thesis, TU Delft, 2003.
- (27) Shen, J.; Chen, X.; Zheng, Y.; Wang, H.; Xu, Z. *J. Phys.: Cond. Matter* **2003**, *15*, 5353. Coleman, R. V.; Eiserman, G.; Everson, M. P.; Johnson, A.; Falicov, L. M. *Phys. Rev. Lett.* **1985**, *55*, 863.
- (28) Adelman, T. L.; McCarten, J.; Maher, M. P.; DiCarlo, D. A.; Thorne, R. E. *Phys. Rev. B* **1993**, *47*, 4033.
- (29) Lemay, S. G.; Thorne, R. E.; Li, Y.; Brock, J. D. *Phys. Rev. Lett.* **1999**, *83*, 2793.
- (30) Mantel, O. C.; Chalin, F.; Dekker, C.; van der Zant, H. S. J. *Synth. Met.* **1999**, *103*, 2612.

NL0480722